

Short Communication

Investigation of 7075 Aluminum Alloy Corrosion in Marine Environment

Huan Sheng Lai^{1,2}, Xiaowei Jiang¹, Huali Li³, Hongyuan Cui³, Zilong Zhao^{3,*}, Hui Guo^{3,*}, Liang Li⁴

¹ Sino-French Institute of Nuclear Engineering and Technology, Sun Yat-sen University, Zhuhai 519082, China

² School of Mechanical and Power Engineering, Nanjing Tech University, Nanjing, 211816, China

³ School of Chemical Engineering and Technology, Sun Yat-sen University, Zhuhai, 519082, China

⁴ School of Physics, Engineering and Computer Science, University of Hertfordshire, UK AL109AB

*E-mail: laihsh@mail.sysu.edu.cn; zhaozlong@mail.sysu.edu.cn; guoh37@mail.sysu.edu.cn

Received: 10 February 2022 / Accepted: 17 March 2022 / Published: 5 April 2022

Aluminum alloys have been widely used in the automotive, marine, and aerospace industries due to lightweight and satisfactory mechanical performance. However, their applications are greatly limited by corrosive-resistance performance. In this work, the corrosion mechanism of 7075 aluminum alloy is systematically investigated in two corrosive marine environments: simulated seawater and real seawater. Results show that the alloy had a faster corrosion rate by yielding much deeper corrosion holes in the real seawater than the simulated media. Moreover, there is a lower corrosion voltage and higher corrosion current in the real sea water, which accounts for the corrosion-resistance performance. In addition, the diverse corrosion products in the real seawater also provide an evidence of different corrosion mechanisms. From these phenomena, it is speculated that the presence of microorganisms in real seawater may lead to microbial corrosion and increase the active sites of the alloy surface, therefore accelerating the local corrosion of the alloy surface.

Keywords: Aluminum alloy, Microbial corrosion, Microstructure, Corrosion product

1. INTRODUCTION

Aluminum alloys are the dominant materials used for airframe structures until the increasing trend in the use of polymer–matrix composites. Compared to other alloys, aluminum alloy shares great advantages in terms of high mechanical strength, lightweight, and ease to process. Currently, the amount of aluminum alloy overweighs plenty of other metals or alloys and is just second to steel [1, 2]. As a typical example, 7075 aluminum alloy has emerged as an important material in the fields of carrier-based aircraft and ships [3-5]. In recent years, the rising CO₂ emissions associated with increasing traffic and transportation have driven the development of enhanced lightweight aluminum alloys for automotive

applications [6-8]. However, there are severe corrosion problems for aluminum alloy in marine environment, making it inferior to other anti-corrosive materials, such as polymeric composite or stainless steel. Therefore, lightweight aluminum alloys with improved corrosion resistance are highly in demand [9,10].

At present, the main strategies of corrosive protections rely on corrosion-resistant materials, surface treatment and modification, coating plating, cathodic protection, corrosion inhibitors, structural health monitoring, and testing, safety evaluation, and reliability analysis, etc. [11-14]. However, the foundation of protection engineering is established on the investigation of the corrosion mechanism of materials in various corrosive environments. Therefore, prior to the discovery of novel aluminum alloy, understanding the corrosion-resistance performance of such alloy in marine environment is highly demanding. In recent years, researchers have found that microbial corrosion is one of the key factors for the corrosion failure of structural materials and components. The loss caused by microbial corrosion in marine environment accounts for more than half of the economic loss [15-17]. However, to the best of our knowledge, the importance of microbial corrosion in 7075 aluminum alloy has not been intensively investigated or conversed confirmed.

In this work, the corrosion mechanism and the evolution of corrosion products of 7075 aluminum alloy are systematically investigated in two corrosive marine environments, e.g. simulated seawater (seawater without adding microorganisms) and real seawater (seawater containing marine microorganisms in the deep sea). It is demonstrated that the corrosion rate of the alloy in real seawater is much higher than that without microbial corrosion in simulated seawater. The lower corrosion voltage and higher corrosion current in the real seawater account for the corrosion difference. Moreover, the difference in corrosion products indicates distinct corrosion mechanisms.

2. EXPERIMENTAL PROCEDURE

Commercial 7075 aluminum alloy plates were cut into corrosion samples with the dimensions of 20×20×10 mm. The samples were polished with 600 # sandpaper firstly and then with 1500 # sandpaper. After that, they were washed with deionized water and air dried. The electrochemical performance was measured after the samples were immersed in seawater for 14 days. The composition of simulated seawater is shown in Table 1, which is in good accordance with real seawater. The real seawater is obtained from the surface sea of Yangjiang, China.

Table 1. Chemical composition of simulated seawater (g/L)

NaCl	MgCl ₂	Na ₂ SO ₄	KCl	H ₃ BO ₃	CaCl ₂	NaHCO ₃	KBr	SrCl ₂	NaF
24.53	5.20	4.09	0.695	0.027	1.16	0.201	0.101	0.025	0.003

The microstructure of samples was examined by a 3D Optical Microscopy (OM, LEICA DVM6) and a Scanning Electron Microscope (SEM, JSM-7800F, JEOL, Japan) equipped with an Oxford electron backscattered diffraction system and Energy Dispersive Spectrometer (EDS). The

electrochemical properties of the as-obtained substrate surface were determined with an electrochemical workstation (C. H., Shanghai), equipped with a standard three-electrode system with an Ag/AgCl reference electrode, a platinum mesh as the counter electrode, and the sample as the working electrode. Phase analysis was carried out on an XPERT-PRO X-ray diffraction (XRD) system with the copper target and the scanning speed of 10 degrees/minute.

3. RESULTS AND DISCUSSION

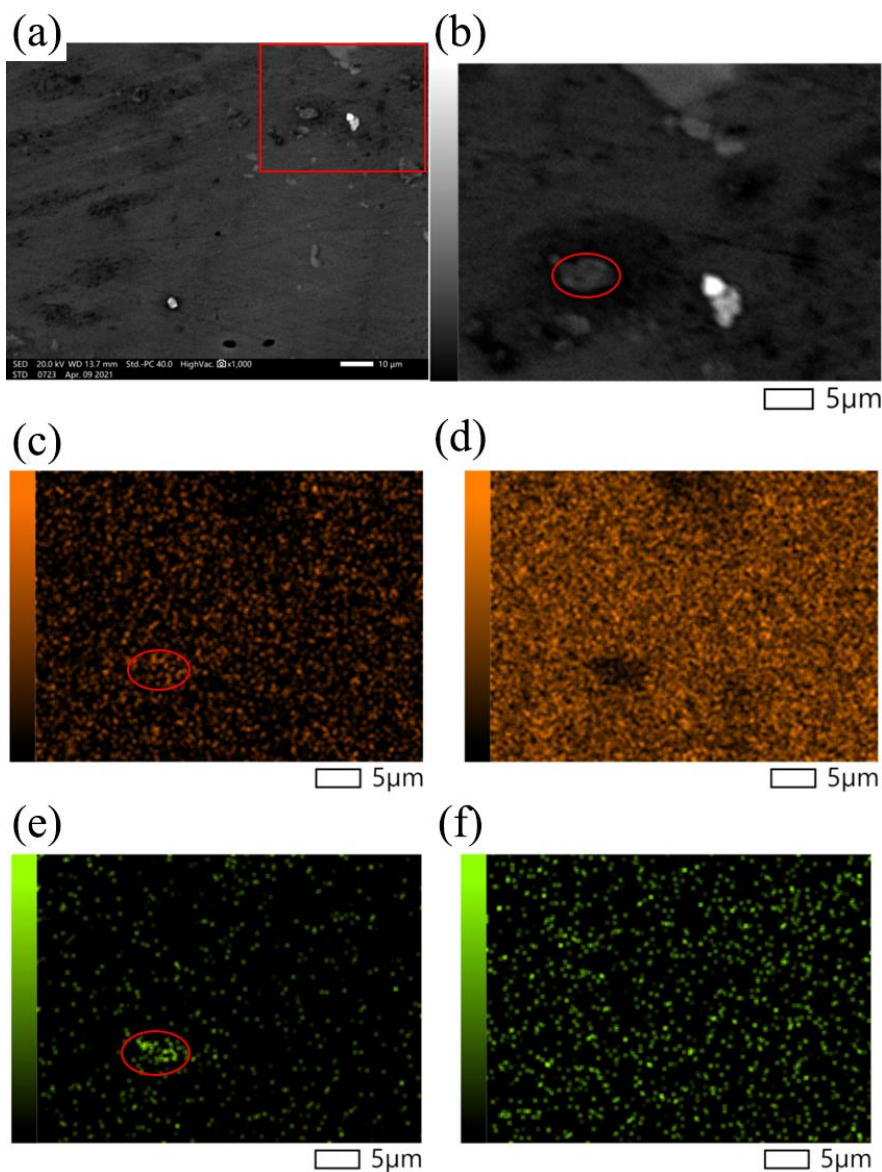


Figure 1. SEM and EDS images of 7075 aluminum alloy: (a) original SEM image, where part of the figure (red border) is zoomed and shown in (b); (c), (d), (e), and (f) EDS mapping of the distribution of Mg, Al, Cu, and Zn elements.

The chemical composition of 7075 aluminum alloy was characterized prior to the corrosion test. The SEM and EDS images of 7075 aluminum alloy are shown in Figure 1. The matrix of the alloy is aluminum and the elements of Mg, Cu, and Zn are uniformly distributed. The positions of Mg and Cu

are basically at the same places, indicating the existence of Mg_2Cu in the alloy. The existence of the second active phase may accelerate the electrochemical corrosion rate in the alloy [18,19]. Since Zn is the main component in 7075 aluminum alloy besides Al element, the uniform distribution of Zn element may contribute to the mechanical performance of alloy by solid solution strengthening.

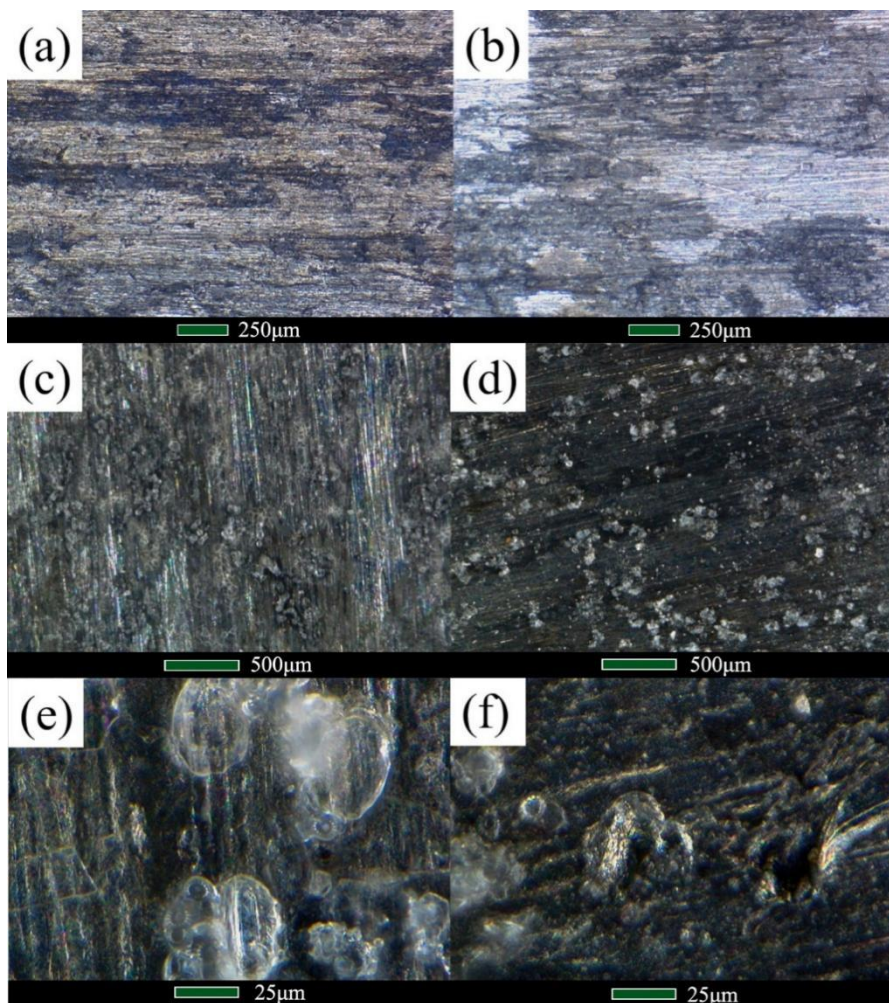


Figure 2. Optical Microscopy images of 7075 aluminum alloy: (a), (c), and (e) are the optical microscopy images after corrosion in simulated seawater; (b), (d), and (f) are the optical microscopy images after corrosion in real seawater.

Subsequently, the 7075 aluminum alloy samples were immersed both in simulated seawater and real seawater for comparison. The corrosion behavior can be monitored through observation of the corrosion morphology [20, 21]. As shown in Figure 2, there is a significant difference in the morphology of 7075 aluminum alloy after being immersed in the two media. In real seawater, there are obvious corrosion holes on the surface, indicating that NaCl and microbial corrosion in real seawater have stronger local corrosion capabilities even with a small amount of NaCl on the surface of 7075 aluminum alloy. By contrast, the NaCl content in the simulated seawater is rather high. As depicted in Figure 2 (e), the surface is mainly corroded by oxygen in presence of Cl^- . While the sample immersed in simulated seawater does not contain microbial, the real seawater contains microbial, which may lead to microbial

corrosion. Indeed, the source battery reaction occurs preferentially at the active sites on the alloy surface, especially in the presence of biological sulfate-reducing bacteria, which could form a galvanic corrosion source battery and accelerate the corrosion of the alloy [22, 23]. A 3D optical microscopic is used to further characterize the corrosion morphology. As shown in Figure 3, the deepest corrosion hole in the simulated seawater is $7.47\ \mu\text{m}$, while this value is as high as $11.22\ \mu\text{m}$ in real seawater.

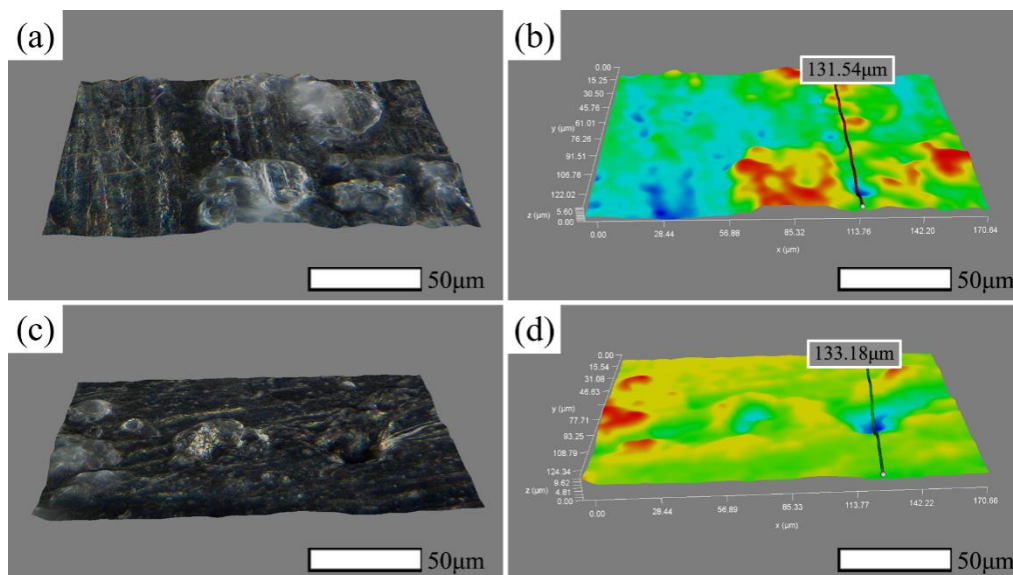


Figure 3. 3D optical microscopy images of 7075 aluminum alloy: (a) optical microscopy image after corrosion in simulated seawater, (b) the 3D reconstruction of (a), (c) optical microscopy image after corrosion in real seawater, (d) the 3D reconstruction of (b).

Electrochemical characterization was also performed to quantitatively characterize the corrosion resistance of 7075 aluminum alloy. As shown in Figure 4 and Table 2, the corrosion voltage is $-0.64\ \text{V}$ in the simulated environment with no microorganisms in the corrosion media. However, the corrosion voltage dropped to $-0.75\ \text{V}$ in the real seawater environment where microorganisms exist. Moreover, compared to that in simulated seawater, there is a much higher corrosion current in the presence of microorganisms. This may be ascribed to increasing the surface active sites of the alloy and accelerates the local corrosion on the surface of the alloy by the presence of microorganisms, which is consistent with the aforementioned analysis results of Figure 2 and Figure 3.

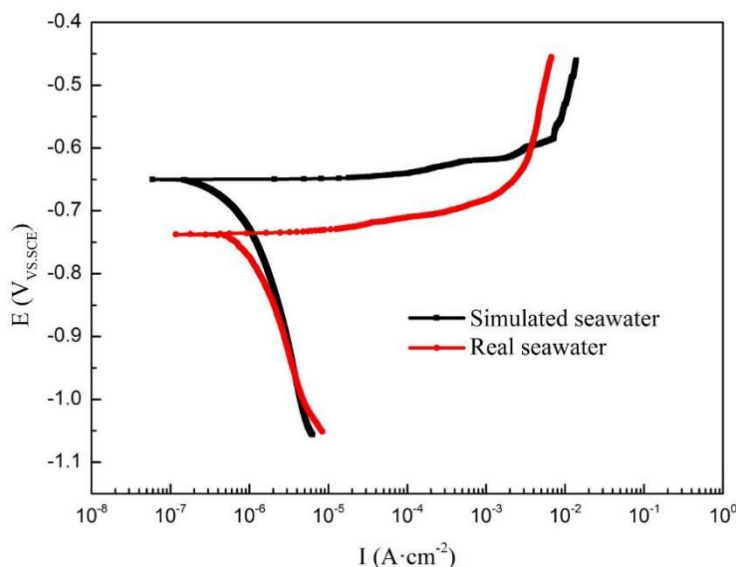


Figure 4. Polarization curves in simulated seawater and real seawater, which measured after immersing 14 days

Table 2. Corrosion potential ($E_{corr.}$) and corrosion current density ($I_{corr.}$) derived from different systems.

	$E_{corr.}$ (V)	$I_{corr.}$ (A cm ⁻²)
Simulated seawater	-0.644	9.6511E-7
Real seawater	-0.753	6.9664E-6

From Figure 5 and Table 3, the impedance value of alloy in real seawater is significantly lower than the sample in the simulated seawater, which indicates that the real seawater is more corrosive. It can be seen from the phase angle diagram that the sample in real seawater has obvious diffusion impedance (W) in the low-frequency region. The appearance of diffusion resistance indicates that the electrode reaction process is controlled by mass transfer and diffusion. The appearance of diffusion usually forms a relatively dense corrosion product film on the surface of the surface electrode [24]. This phenomenon correspondingly results in a faster corrosion rate of the metal in the surface anode seawater medium, which accelerates the formation of the surface corrosion product film. Indeed, the existence of microorganisms accelerates the corrosion of aluminum alloy, as the microbial corrosion is one of the important corrosion factors for metal. It can be seen from the Fig.5a that as the corrosion time increases, the impedance of 7075 aluminum alloy becomes smaller and smaller, while the impedance in Fig.5b increases as the corrosion time increases. The main reason for this difference is that the real seawater contains microorganisms and may destroy the formation of the oxide film, while there is no microorganism in the simulated seawater, and the aluminum alloy forms a dense oxide film, which increases the resistance value of the alloy.

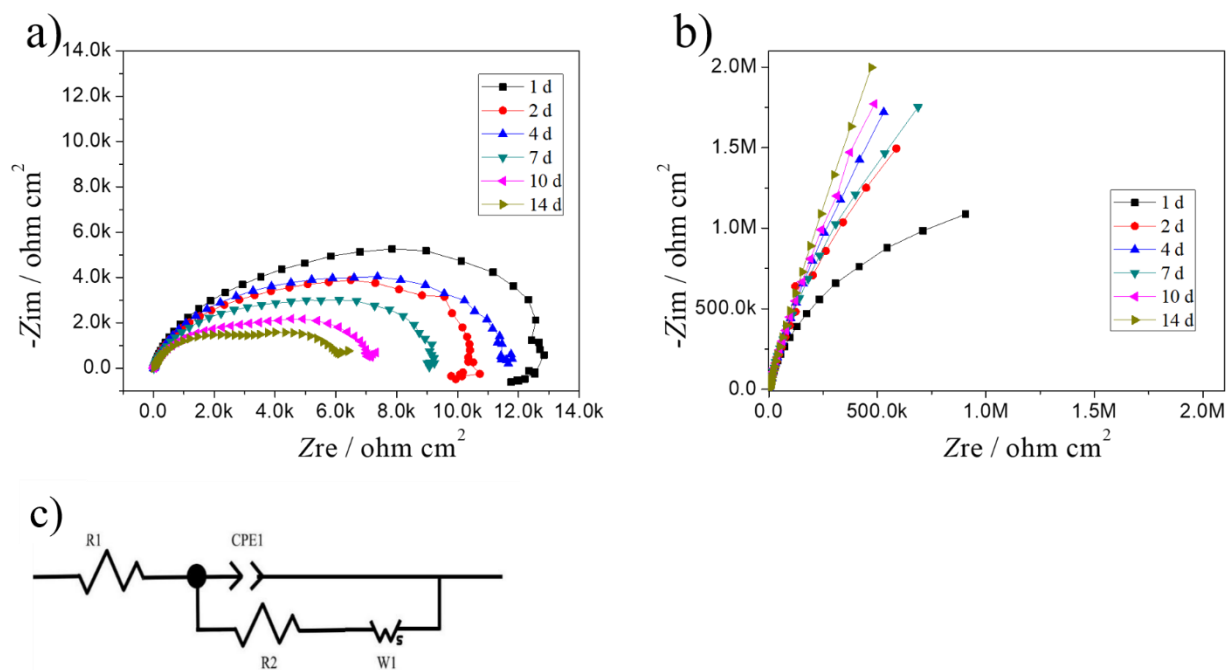


Figure 5. (a) EIS experimental results of 7075 aluminum alloy in real seawater for 14 day (b) EIS experimental results of 7075 aluminum alloy in simulated seawater for 14 day (c) Scheme of the equivalent circuits applied to fit EIS plots. R1 is the internal resistance of the seawater itself, R2 is the internal resistance of the container, and CPE1 is the constant phase element impedance at the interface between the seawater and the container

Table 3. Fitted parameters for EIS spectrum depicted in Figure 5a and Figure 5b.

	R_s (Ω cm ²)	CEP-T (Ω^{-1} cm ⁻²)	CEP-P	R_t (Ω cm ²)
Real seawater 1d	12.1	9.4E-6	0.85	1.45E4
2	12.3	3.2E-6	0.82	1.11E4
4	11.7	4.8E-6	0.77	1.23E4
7	12.2	2.8E-6	0.79	9.26E3
10	13.2	2.3E-6	0.78	7.93E3
14	11.8	1.5E-6	0.85	6.83E3
Simulated seawater 1d	11.3			
2	12.1	1.23E-5	0.95	2.3E6
4	11.4	1.45E-5	0.91	4.5E8
7	11.5	2.71E-5	0.89	8.9E8
10	12.5	2.88E-5	0.92	3.9E9
14	12.5	3.21E-5	0.90	9.6E9

To further investigate the morphology and phase composition of corrosion products, SEM analysis is conducted on the corrosion products of 7075 aluminum alloy. From Figure 6 (a) and (c), a certain corrosion product film is formed on the surface of the alloy in the simulated seawater corrosion environment, and the product is relatively dense without obvious cracks. In contrast, as shown in Figure 6 (b) and 6 (d), there are obvious cracks on the surface of the alloy in real seawater, and the corrosion products cannot protect the alloy from further corrosion.

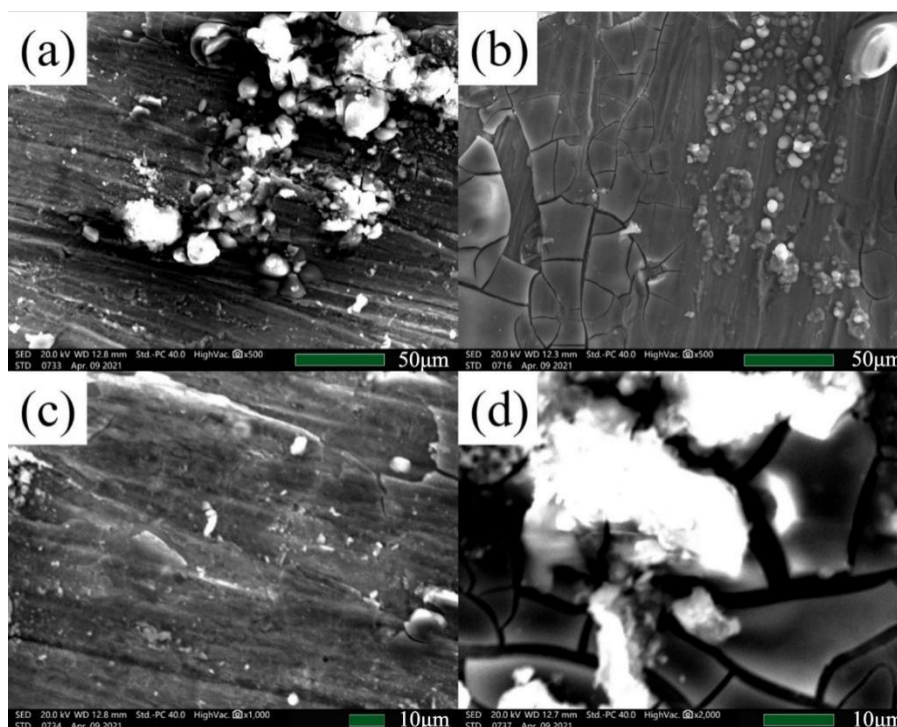


Figure 6. SEM image of 7075 aluminum alloy: (a) and (c) are the microscopic images after corrosion in simulated seawater, (b) and (d) are the microscopic images after corrosion in real seawater.

In the following, Energy Dispersive Spectrometer (EDS) is applied to explore the corrosion products of aluminum alloy in the simulated seawater and real seawater. The magnesium on the surface of 7075 aluminum alloy in the simulated seawater is much higher than the product in the real seawater (Figure 7 (a)). On the contrary, the content of C and O in the corrosion products on the alloy surface increase significantly, indicating that microorganisms participated in the corrosion process in the real seawater where microorganisms exist (Figure 7 (b)). This phenomenon implies that in the absence of microorganisms, oxide films such as $Mg(OH)_2$ and Al_2O_3 can be formed on the surface of the alloy to prevent further corrosion. Nevertheless, the Mg element is an important element for the survival of microorganisms and organisms. Therefore, in a corrosive environment with microorganisms, magnesium becomes an active site for microorganisms to absorb nutrients. Corrosion occurs preferentially in areas where magnesium is distributed, thereby accelerating the corrosion of 7075 alloys in the marine microbial corrosion environment [25].

Moreover, X-Ray Diffraction (XRD) tests have been performed on the samples. As shown in Figure 8, there is no obvious difference between the two samples in terms of product phase types. At the same time, the signals of corrosion product in real seawater at 13, 17, and 65 degrees are significantly stronger than the corrosion product in simulated seawater. As corrosion products are formed more thoroughly in real seawater, the crystal peaks of the products are stronger. In addition, the corrosion products of real seawater at 44 degrees have a new peak, indicating that there are slightly more types of corrosion products in the microbial corrosion environment. Therefore, microbial corrosion may be the key bottleneck for the application of 7075 aviation super-aluminum alloy in seawater corrosion [26].

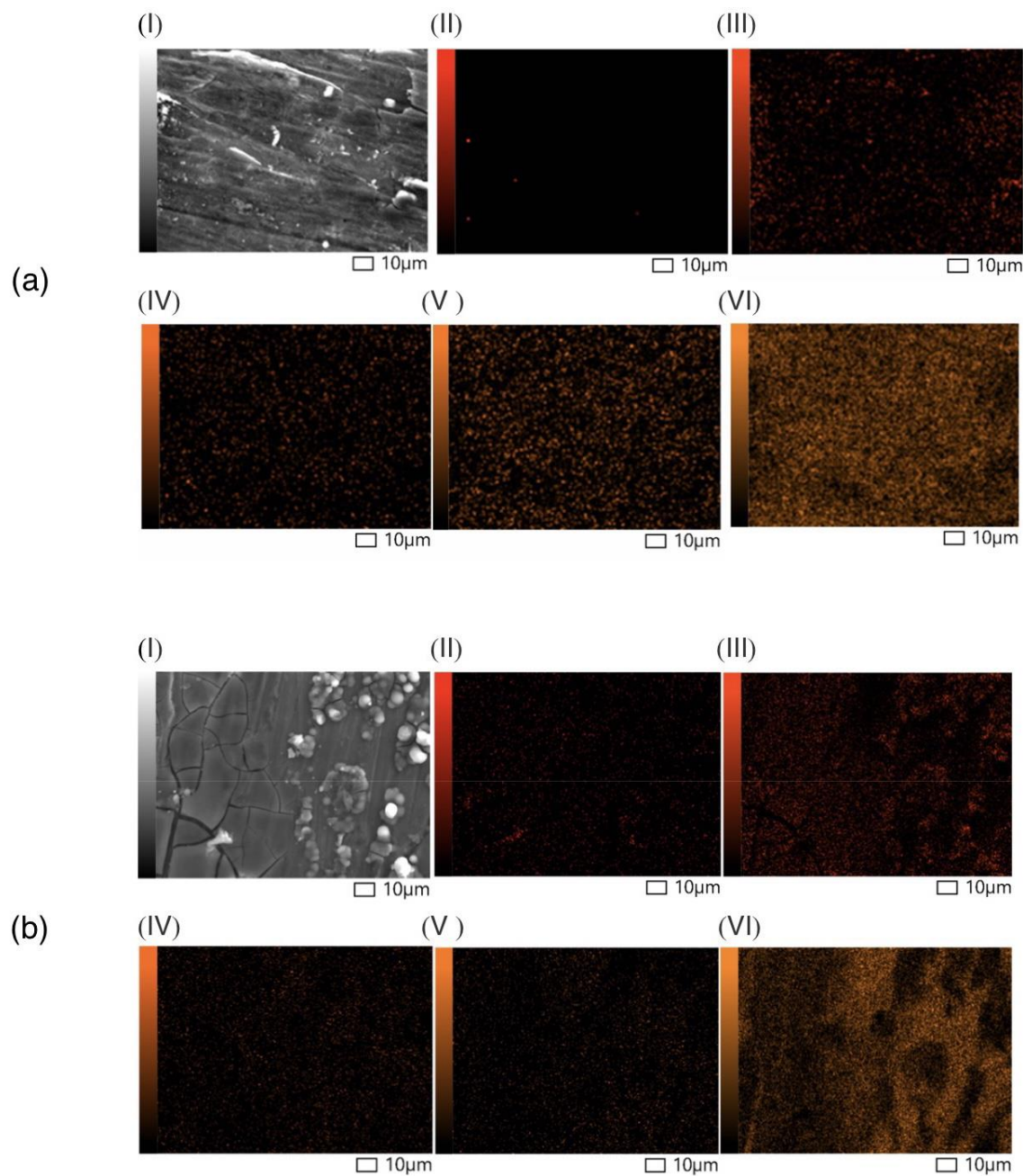


Figure 7. EDS images of 7075 aluminum alloy after corrosion in simulated seawater (a) and in real seawater (b). (I) original SEM image, (II) C element, (III) O element, (IV) Na element, (V) Mg element, (VI) Al element.

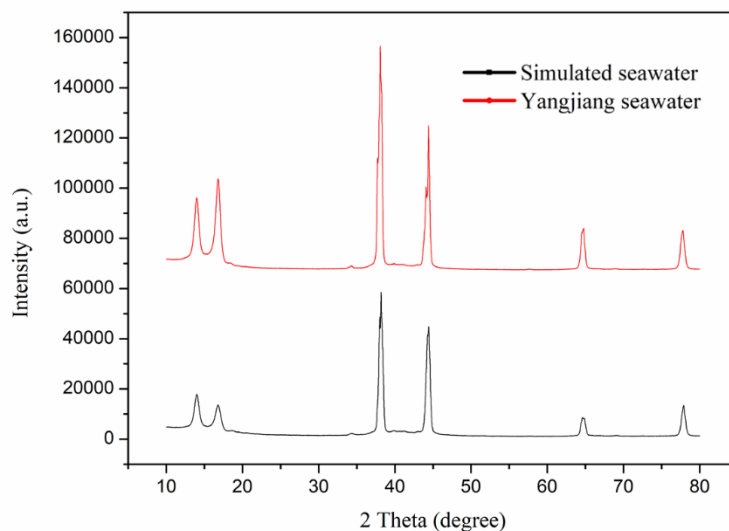


Figure 8. XRD (X-Ray Diffraction) pattern of 7075 aluminum alloy after corrosion in simulated seawater and real seawater with 10-80 degrees of copper target

4. CONCLUSION

In this work, the corrosion performance of 7075 aluminum alloy is systematically investigated in simulated seawater and real seawater. Although both media contain comparable chemical ingredients, the absence of microorganisms in simulated seawater may induce a huge difference in corrosion performance. From optical and electronic microscopic observation, the corrosion rate in real seawater leads to larger and deeper corrosion holes than that in simulated seawater, emphasizing the important influence of corrosion media. Similarly, the electrochemical impedance measurement also confirms the difference in corrosion rate. The lower corrosion voltage, as well as the much higher corrosion current, indicate the strong influence of the microorganisms. Moreover, the diverse corrosion products in the real seawater corrosive environment also provide the evidence of different corrosion mechanisms. This work may clear up the doubt of corrosion media influence in 7075 aluminum alloy and endow the alloy with better anti-corrosion performance in the marine environment in the future.

ACKNOWLEDGEMENTS

This work was supported by the Jiangsu Province Key Laboratory of Industrial Equipment Manufacturing and Digital Control Technology.

References

1. M.C. Reboul, B. Baroux, *Mater. Corros-Werkst. Korros.*, 62(3) (2011) 215-233.
2. R. Arrabal, B. Mingo, A. Pardo, M. Mohedano, E. Matykina, I. Rodriguez, *Corrosion Sci.*, 73 (2013) 342-355.
3. S. Chayong, H.V. Atkinson, P. Kapranos, *Mat Sci Eng A-Struct.*, 390(1-2) (2005) 3-12. (in

- English)
4. J. Bi, Z.L. Lei, Y.B. Chen, X. Chen, Z. Tian, J.W. Liang, X.R. Zhang, X.K. Qin, *Mat Sci Eng A-Struct.*, 768 (2019) 9, 138478. (in English)
 5. A. Baradeswaran, A.E. Perumal, *Compos. Pt. B-Eng.*, 56 (2014) 464-471. (in English)
 6. L. Stemper, M.A. Tunes, P. Dumitraschkewitz, F. Mendez-Martin, R. Tosone, D. Marchand, W.A. Curtin, P.J. Uggowitzer, S., *Acta Mater.*, 206 (2021) 116617.
 7. J. Hirsch, *Trans. Nonferrous Met. Soc. China.*, 24(7) (2014) 1995-2002
 8. J. Hirsch, *Mater. Trans.*, 52(5) (2011) 818-824.
 9. J. Bhandari, F. Khan, R. Abbassi, V. Garaniya, R. Ojeda, *J. Loss Prev. Process Ind.*, 37 (2015) 39-62.
 10. B. Hou, D. Zhang, P. Wang, *BCAS.*, 31(12) (2016) 1326-1331, 1000-3045.
 11. G. Zhang, L. Wu, A. Tang, H. Pan, Y. Ma, Q. Zhan, Q. Tan, F. Pan, A. Atrens, *J. Electrochem. Soc.*, 165(7) (2018) C317-C327.
 12. K.K. Ma, H.M. Wen, T. Hu, T.D. Topping, D. Isheim, D.N. Seidman, E.J. Lavernia, J.M. Schoenung, *Acta Mater.*, 62 (2014) 141-155. (in English)
 13. J.H. Martin, B.D. Yahata, J.M. Hundley, J.A. Mayer, T.A. Schaedler, T.M. Pollock, *Nature*, 549(7672) (2017) 365-369. (in English)
 14. Y.B. Yan, Z.W. Zhang, W. Shen, J.H. Wang, L.K. Zhang, B.A. Chin, *Mat Sci Eng A-Struct.*, 527 (9) (2010) 2241-2245. (in English)
 15. R. Jia, J.L. Tan, P. Jin, D.J. Blackwood, D. Xu, T. Gu, *Corrosion Sci.*, 130 (2018) 1-11.
 16. Y. Li, D. Xu, C. Chen, X. Li, R. Jia, D. Zhang, W. Sand, F. Wang, T. Gu, *J. Mater. Sci. Technol.*, 34(10) (2018) 1713-1718.
 17. T. Liu, S. Pan, Y. Wang, Z. Guo, W. Wang, Q. Zhao, Z. Zeng, N. Guo, *Corrosion Sci.*, 162 (2020) 108215.
 18. Z. Zhao, Y. Liu, Y. Zhong, X. Chen, Z. Zhang, *Int. J. Electrochem. Sci.*, 13(5) (2018) 4338-4349.
 19. Z. Zhao, Z. Sun, W. Liang, Y. Wang, L. Bian, *Mat Sci Eng A-Struct.*, 702 (2017) 206-217.
 20. F. Liu, J. Zhang, C. Sun, Z. Yu, B. Hou, *Corrosion Sci.*, 83 (2014) 375-381.
 21. H. Liu, B. Zheng, D. Xu, C. Fu, Y. Luo, *Ind Eng Chem Res.*, 53(19) (2014) 7840-7846.
 22. H.W. Liu, Y.F. Cheng, D.K. Xu, H.F. Liu, *J. Electrochem. Soc.*, 165(7) (2018) C354-C361.
 23. M. Siva Surya, G. Prasanthi, *Adv. Mater. Process. Technol.*, (2020) 1-16.
 24. H. Liu, D. Xu, K. Yang, H. Liu, Y.F. Cheng, *Corrosion Sci.*, 132 (2018) 46-55.
 25. H. Liu, T. Gu, G. Zhang, H. Liu, Y.F. Cheng, *Corrosion Sci.*, 136(2018) 47-59.
 26. H. Liu, Y.F. Cheng, *Electrochim. Acta*, 266 (2018) 312-325.